PORE-SCALE SIMULATION OF NMR RESPONSE IN CARBONATES

Olumide Talabi[1], Saif Alsayari[1], Martin A. Fernø[2], Haldis Riskedal[2], Arne Graue[2] and Martin J Blunt[1]
[1] Department of Earth Science and Engineering, Imperial College London, UK
[2] Department of Physics and Technology, University of Bergen, Norway

This paper was prepared for presentation at the International Symposium of the Society of Core Analysts held in Abu Dhabi, UAE 29 October-2 November, 2008

ABSTRACT

We simulate magnetization decay in porous media using a random walk method. Simple sand pack systems were initially studied before actual porous and heterogeneous carbonates were investigated. Topologically equivalent sand pack networks were extracted from micro-CT images using a maximal ball algorithm. The simulated magnetization decay and T_2 distribution in the images and networks were successfully compared with experimental data. The algorithm used in the simulations of NMR response in networks was validated using a tuned Berea network that reproduced experimental capillary pressure data in Bentheimer sandstone. The simulated magnetization decay and T_2 distribution of this tuned network is shown to be in good agreement with experimental measurements. Significant differences were observed between the simulated magnetization decays of the micro-CT image and extracted network of carbonates. The coincidence between simulated and experimental magnetization decays and T_2 distributions improved when networks are generated from capillary pressure data.

INTRODUCTION

Rock flow properties are usually predicted using a 3D representation of the rock microstructure, which is commonly obtained from X-ray computed tomography (micro-CT) at resolutions of a few microns (Hazlett, 1995; Arns et al., 2004). In carbonate rocks however, because of the bimodal pore size distributions (micro-pores and macro-pores), with micro pores having sizes in sub-micron range, micro-CT resolutions of a few microns cannot capture the features of these micro pores. In order to overcome this limitation, multiple point statistics had been used to reconstruct 3D images of carbonates from 2D thin section images (Okabe and Blunt, 2004; Okabe and Blunt, 2005). Predictions of transport properties such as permeability, formation factor, relative permeability and capillary pressures have been made on networks extracted from these reconstructed 3D images of carbonates using a maximal ball algorithm (Al-Kharusi and Blunt, 2007). An alternative to generating networks without an underlying microstructure is by tuning the properties of a known network to generate simulated capillary pressures that reproduces the measured data, (Valvatne and Blunt, 2004).

In this work, we obtained a micro-CT image of a carbonate and used a maximal ball algorithm (Silin et al., 2003; Silin and Patzek, 2006; Al-Kharusi and Blunt, 2007; Dong, 2007) to extract a network of pores and throats. We simulated magnetization decay in the image and network using a random walk method, (Ramakrishnan et al., 1999; Øren et al., 2002), these decays were inverted into T_2 distributions by a curvature-smoothing regularization method (Chen et al., 1999; Toumelin, 2002). We observed significant differences in the simulated magnetization decays of the image and network, inferring that the network is not identical both in the geometry of the network elements and topology to the micro-CT image. To overcome this problem, we generated networks that reproduce the mercury injection capillary pressure data of the carbonates studied in this work. An important parameter in the simulation of NMR response is surface relaxivity; the values used in our simulations are within the range measured previously for carbonates. Simulation results of the magnetization decays and T_2 distributions of the resulting networks were compared with experimental measurements.

SIMULATION OF NMR RESPONSE

NMR response is simulated in the 3D images and networks by the random walk method (Ramakrishnan et al., 1999; Øren et al., 2002). This method simulates the Brownian motion of a diffusing particle called the walker. Initially the walkers are placed randomly in the 3D pore space, at each time step they diffuse from their current position $[x(t), y(t), z(t)]$ to a new position $[x(t+\Delta t), y(t+\Delta t), z(t+\Delta t)]$ on the surface of a sphere with radius s, centered on their initial positions. The time step Δt is given by:

$$\Delta t = \frac{s^2}{6D} \tag{1}$$

where D is the diffusion coefficient of the fluid, the new position after each time step is given by:

$$x(t+\Delta t) = x(t) + s\sin\phi\cos\theta \tag{2}$$

$$y(t+\Delta t) = y(t) + s\sin\phi\sin\theta \tag{3}$$

$$z(t+\Delta t) = z(t) + s\cos\phi \tag{4}$$

the angles θ and ϕ are randomly selected in the range $(0 \le \theta \le 2\pi)$. If the walker encounters a solid surface, it is killed with a finite killing probability, δ (Bergman et al., 1995):

$$\delta = \frac{2\rho s}{3D} \tag{5}$$

where ρ is surface relaxivity. If the walker survives, it simply bounces off the solid surface and returns to its previous position and time is advanced by the time step given in equation (1). When a walker in a micro-CT image diffuses out of the entire image, a new walker is placed in a randomly selected pore voxel on the opposite face of the image thereby leading to a conservation of the total number of walkers in the image at any given time. For walkers in networks, inter pore diffusion (pore-to-throat and throat-to-pore) was

accounted for, as such walkers in an element always diffuse into connected elements when their z-coordinates are negative or greater than the length of the element, except for isolated pores where all the walkers decay within the pore. The life time distribution of the walkers is the magnetization decay which is inverted into T_2 distribution by using the curvature-smoothing regularization method (Chen et al., 1999; Toumelin, 2002).

RESULTS AND DISCUSSION

NMR simulations were performed on 3D images and extracted networks of sand packs (cores LV60B and F42B) and networks generated from the experimental capillary pressure measurements of Bentheimer sandstone, Edward limestone (cores MB03 & MB11), and carbonates C22 and C32. Each core used in the study, with corresponding experimental and predicted porosities and permeabilities are listed in Table 1. The brine used to saturate the cores for the NMR experiments have densities and viscosities in the range (1005 – 1050) kg/m^3 and (1.04 – 1.09)×10^{-3} Pa.s respectively.

		Experimental		Network Simulations	
Rock Description	**Core ID**	**Porosity [%]**	**Permeability [mD]**	**Porosity [%]**	**Permeability [mD]**
Sand packs	LV60B	37.0 ± 0.2	(32.2 ± 0.3)×10^3	36.8	29.0×10^3
	F42B	35.4 ± 1.3	(42.0 ± 4.0)×10^3	33.3	48.0×10^3
Bentheimer	-	23.0 ± 0.4	1,410 ± 28	23.0	950
Edwards Limestone	MB03	14.3 ± 0.2	5.3 ± 0.2	14.2	0.2
	MB11	12.4 ± 0.2	5.6 ± 0.2	12.4	2.21
Carbonate Rock	C1	14.8*	72.0*	14.8	167.0
	C22	27.5 ± 0.2	6.6 ± 0.2	27.5	0.03
	C32	29.6 ± 0.2	7.7 ± 0.2	29.6	0.01

* Value determined from micro-CT image

Table 1. Experimental and computed rock properties

Sand Packs

Two quartz sands (Leavenseat sand [LV60B], WBB Minerals, UK and Ottawa unground silica [F42B], US Silica Company) were used for the NMR measurements and micro CT imaging. The micro-CT imaging was performed on small sand pack samples of diameter 0.65 cm and 4 cm in length. The micro-CT imaging was performed on a commercial XMT unit (*Phoenix—X-ray Systems and Services GmbH*), and are shown in Figure 1.Analysis of the resultant image confirms that the sand packs had similar porosities as the plugs used in the NMR experiments. Central cubic sections of voxel sizes 338^3 and 300^3 cropped from the micro CT images of Leavenseat and Ottawa sand packs respectively, were used for the simulations. In the NMR measurements, the sands were packed in cylindrical thermo-plastic sleeve of diameter 3.81 cm and 10 cm in length, these packs were then saturated with brine of viscosity 1.04×10^{-3} Pas and density 1035 kg/m^3. The measurements were performed using a MARAN2 bench top spectrometer (Resonance Instruments) at a temperature of 308K operating at 2 MHz.

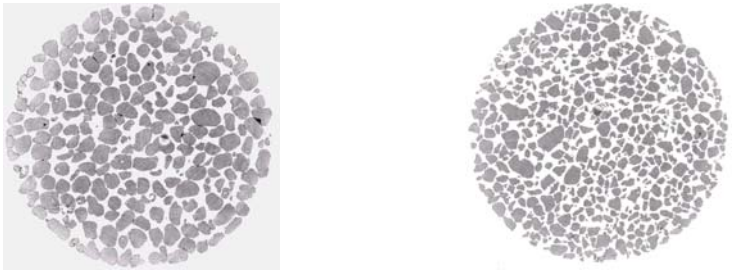

(a) (b)

Figure 1. 2-D micro-CT image of the two quartz sand types used (a) Ottawa unground silica (F42B) with resolution 10 µm and (b) Leavenseat sand (LV60B) with resolution 8.85 µm

The Carr-Purcell-Meiboom-Gill (CPMG) sequence was used for T_2 measurements with an inter-echo spacing of 200µs. A surface relaxivity value of 41×10^{-6} m/s was used in the simulations to match the experimental NMR measurements of both sand packs shown in Figures 2 and 3. This value is higher than reported surface relaxivity for silica sands (Hinedi et al., 1997) which is in the range of 2.89 to 3.06 µm/s.

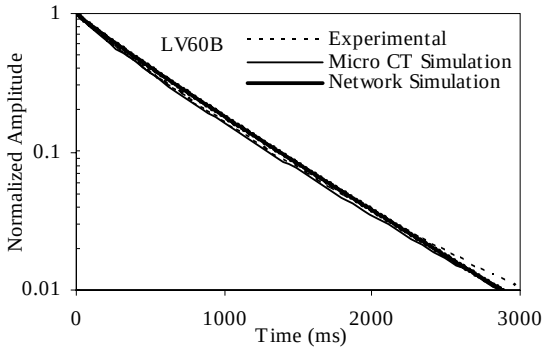

Figure 2a: Comparison of the experimental magnetization decay of LV60B with the micro CT image and extracted network simulations.

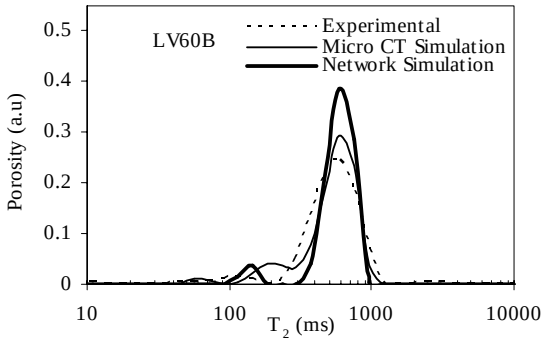

Figure 2b: Comparison of the inverted T_2 distributions from the magnetization decays of LV60B in Figure 2a, porosity (arbitrary unit) is plotted against T_2.

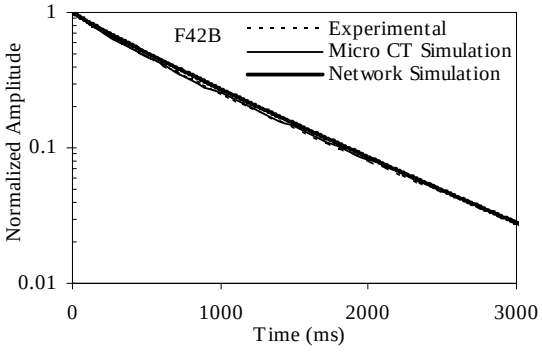

Figure 3a: Comparison of the experimental magnetization decay of F42B with the micro CT image and extracted network simulations.

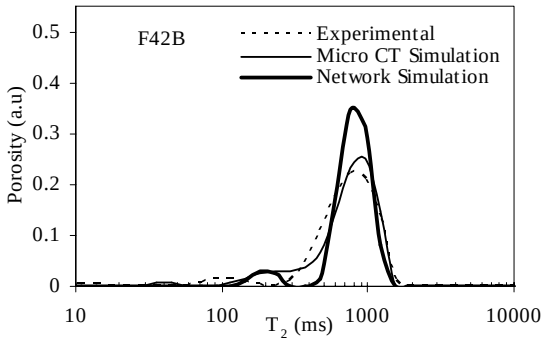

Figure 3b: Comparison of the inverted T_2 distributions from the magnetization decays of F42B in Figure 3a

These earlier reported values were obtained using nitrogen absorption method, which probes the surface area at a much higher resolution, resulting in a larger measured surface area per unit volume and lower surface relaxivity. In our work however, the surface area was determined at the resolution of the micro-CT image (~10μm), resulting in a lower surface area and consequently higher surface relaxivity. The simulated magnetization decays and T_2 distributions of the micro-CT image and network shown in Figures 2 and 3 are somewhat similar. Although, the T_2 distribution of the network is narrower than the micro-CT, which implies that some features of full ranges of pore sizes and shapes are lost in the extraction algorithm.

Bentheimer Sandstone

Simulated NMR results were compared with the experimental NMR data of Bentheimer sandstone to further validate the algorithm used in simulating NMR response in networks. Unlike the sand packs, where a network was extracted from a micro-CT image, the Bentheimer network was generated from a tuned Berea network. A Berea network of 12,349 pores and 26,146 throats with an average coordination number of 4.2 extracted from reconstructed Berea sandstone (Lerdahl et al., 2000) was tuned to match the mercury injection capillary pressure data of Bentheimer sandstone as shown in Figure 4. The underlying assumption of this tuning method is that higher order topological information, are important and less specific to a given system than are properties such as pore size distribution. By preserving the rank order of the individual network elements, topological information are maintained, (Valvatne and Blunt, 2004) thereby resolving the problem of non-uniqueness as noted by Vogel (2000). Relative permeabilities of an intergranular carbonate had been predicted from a network obtained by tuning Berea network elements' properties, these predictions had been successfully compared with experimental results (Valvatne and Blunt, 2004). Simulation of NMR response on the networks obtained using this method is similar to the networks obtained from the maximal ball network extraction algorithm.

The measured capillary pressure data in pore throat radii and the fraction of pore space occupied by the invading fluid is used as input into the tuning algorithm. The initial network elements are assigned pore sizes (radii) based on the radii distribution from the measured capillary pressure data. This tuned network is then used to generate a capillary pressure curve which is compared with the measured capillary pressure data. If no satisfactory match is obtained, the network elements' radii are tuned until the best possible match with the experimental capillary pressure data is obtained. The topological information of the initial Berea network (number of network elements, relative pore locations and connection numbers) are maintained in the tuned network. Pore and throat volumes of the initial Berea network elements were adjusted by a constant factor to obtain the porosity of the experimental data. The surface areas (which are dependent on shape factors) of the tuned network are retained from the initial network. The initial Berea network has a porosity of 18.3% and permeability of 2670mD. The tuned network was then used for the simulation of NMR response which was compared with experimental measurements.

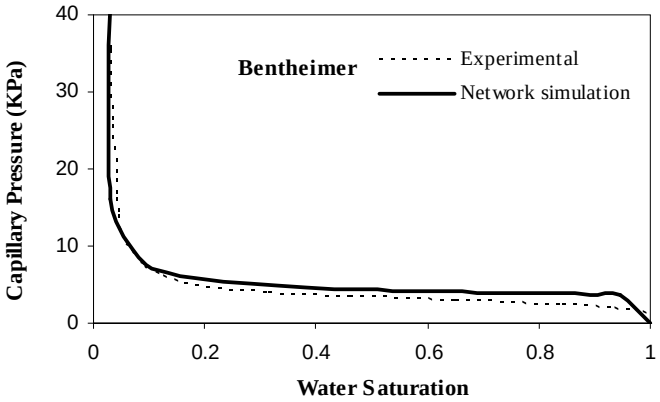

Figure 4: Comparison of the experimental capillary pressure data of the Bentheimer sandstone with simulation results of the tuned Berea network

A Bentheimer sandstone plug of diameter 3.73cm and length 6.01cm fully saturated with brine was used for the NMR measurements. The computed and measured porosities and permeabilities are shown in Table 1. The surface relaxivity used in the simulation was 9.3μm/s, a value obtained for Bentheimer sandstones (Liaw et. al, 1996). Thin-section analysis of the Bentheimer sandstone used for the determination of this surface relaxivity indicates the presence of abundant primary intergranular pores and less abundant secondary pores. The simulated magnetization decay is consistent with experimental values as shown in Figure 5a. The inverted T_2 distributions shown in Figure 5b are similar, indicating that the network fully captured the pore size distribution and topology of the Bentheimer sandstone. These results validate the algorithm used for the simulation of magnetization decay in networks.

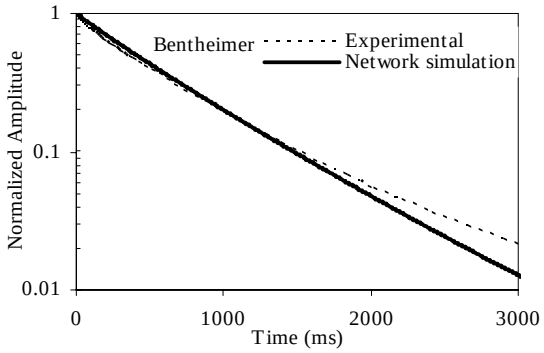

Figure 5a: Comparison of magnetization decays of the experimental data of Bentheimer sandstone with simulation results of the tuned network.

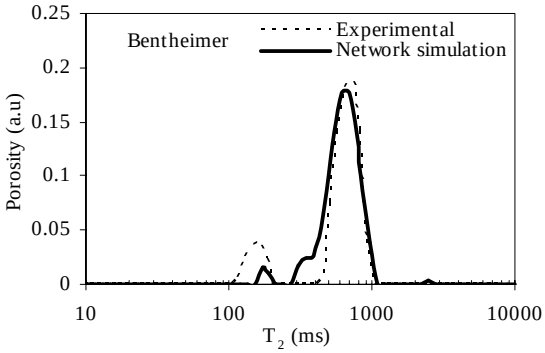

Figure 5b: The inverted T_2 distributions from the magnetization decays of Bentheimer sandstone shown in Figure 5a.

Carbonate Rock Type: C1

Carbonate C1 is a typical calcrete or lithified paleosol, enclosing carbonate clastic detritus Analysis of its thin-section images suggests it probably developed as a weathering rind of limestones during exposure (uplift or sea-level drop). The porosity of its micro CT image

shown in Figure 6 is 14.8% while its resolution is 5.345μm. This carbonate has highly heterogeneous pore structure with poorly connected pores as shown in Figure 6.

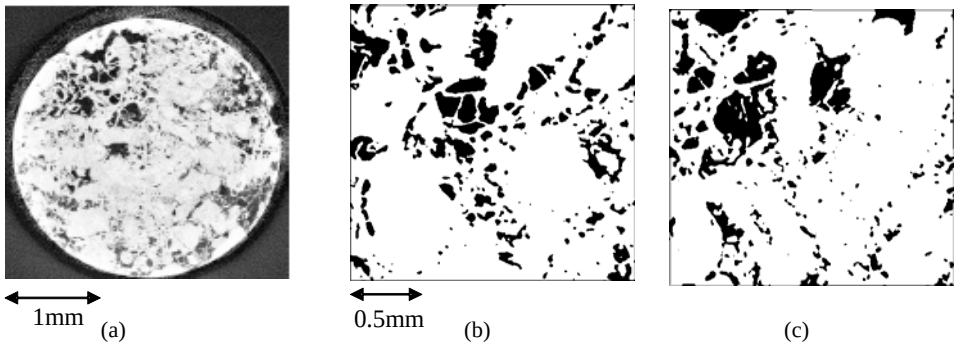

Figure 6: (a) 2D section of the micro-CT image of carbonate C1. (b & c) 2D images of the cropped section from the image in (a); simulations were performed on the 3D cropped section (*the dark areas are the pore spaces and the white represent grains*).

A network of 3,574 pores and 4,198 throats with an average coordination number of 2.3 was extracted from the cropped central cubic section of the micro-CT image using the maximal ball algorithm. This relatively low coordination number is as a result of a large number of poorly connected pores seen in Figure 6. A surface relaxivity of 5μm/s, which is a typical value for carbonates, was used in the simulations. The simulated magnetization of the network decays faster than that of the micro-CT image as shown in Figure 7a. This could be explained by the poorly connected pores and low average coordination number of the network. These results show that network did not fully capture both the geometries of the pores and the topology of the micro-CT image, thereby necessitating the need for alternative methods of generating networks for carbonates.

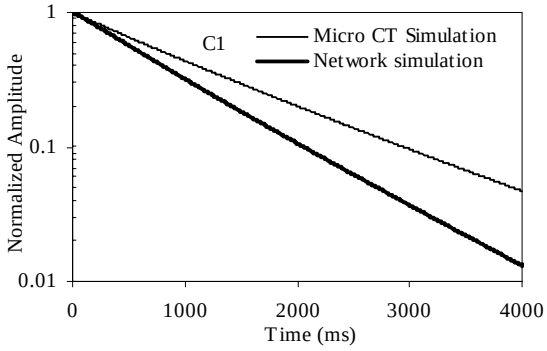

Figure 7a: Comparison of the magnetization decays of the micro CT image of carbonate C1 and the extracted network.

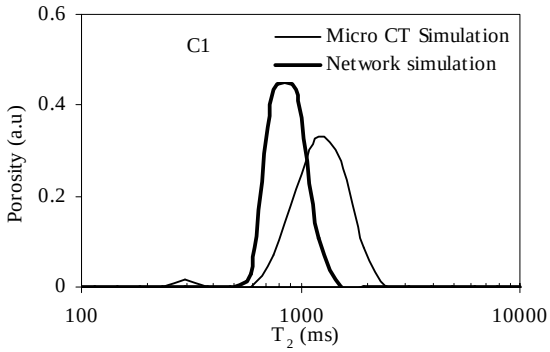

Figure 7b: Comparison of the inverted T_2 distributions of the magnetization decays of carbonate C1 shown in Figure 7a.

Edwards Limestone

Experimental NMR measurements and mercury injection capillary pressure curves were generated on two Edward limestone cores, MB03 and MB11. Core plugs diameter and length was 3.81cm and 6cm, respectively. The computed and measured porosities and

permeabilities are shown in Table 1. The properties of the Berea network were tuned to obtain the best possible match with the limestone mercury injection capillary pressure data of the plugs as shown in Figures 8 and 9.

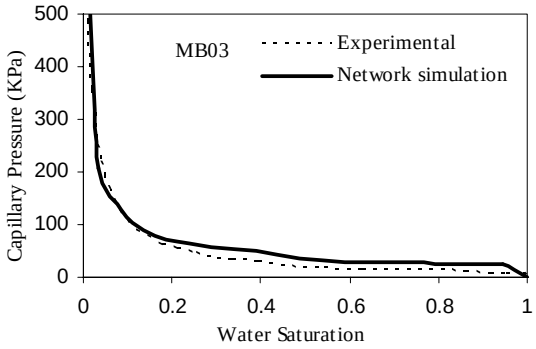

Figure 8: Comparison of the measured capillary pressure curve of MB03 with simulation results of the tuned network.

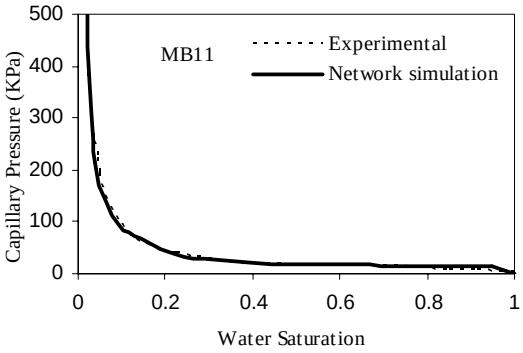

Figure 9: Comparison of the measured capillary pressure curve of MB11 with simulation results of the tuned network.

The resulting tuned networks were then used for the simulations of NMR response which were compared with experimental measurements in Figures 10 and 11. The surface relaxivities used in the simulations were selected to match the experimental data, surface relaxivity values of 3μm/s and 4.5μm/s were used for MB03 and MB11 simulations respectively. These values are within the range for carbonates, usually between 1μm/s and 10μm/s (Chang et al., 1997; Ramakrishnan et al., 1999).

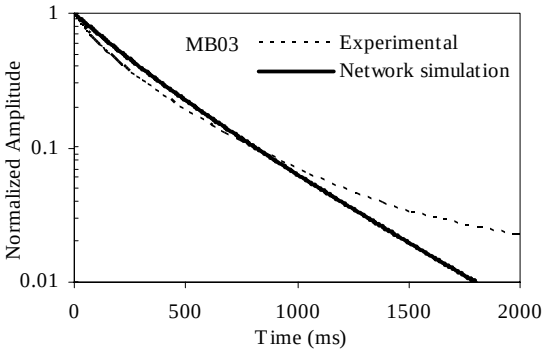

Figure 10a: Comparison of magnetization decays of the experimental data of MB03 with simulation results of the tuned network.

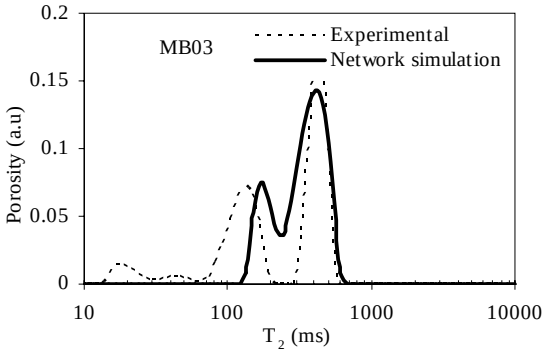

Figure 10b: The inverted T_2 distributions from the magnetization decays of MB03 shown in Figure 10a.

Although surface relaxivity values were selected to match experimental data, the magnetization decays faster in the network than experimental observations at late times, shown in Figures 10a and 11a. Similar trends were observed in the T_2 distributions shown in Figures 10b and 11b, although the T_2 distributions of the networks seem to be wider than the experimental data.

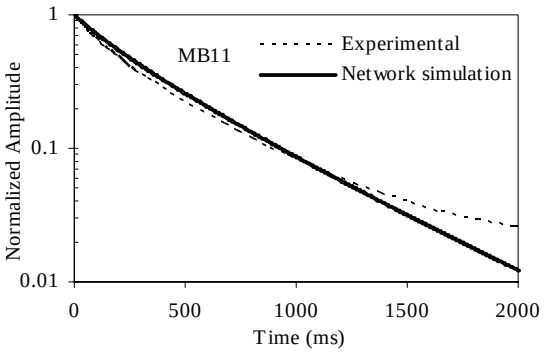

Figure 11a: Comparison of magnetization decays of the experimental data of MB11 with simulation results of the tuned network.

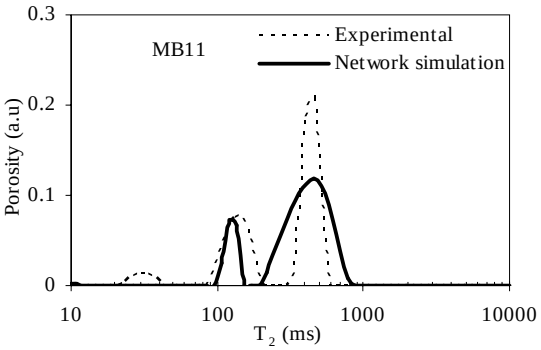

Figure 11b: The inverted T_2 distributions from the magnetization decays of MB11 shown in Figure 11a.

Carbonates: C22 & C32

NMR and mercury injection capillary pressure measurements were also performed on two homogeneous carbonate reservoir core samples (C22 and C32) from a producing field in the Middle East. Core plug diameter and length was 3.81cm and 10cm, respectively for both cores during NMR measurements. The computed and measured porosities and permeabilities are shown in Table 1. A similar approach to the Edward limestone was selected, where the properties of the Berea network were tuned to match the mercury injection capillary pressure data, shown in Figures 12 and 13.

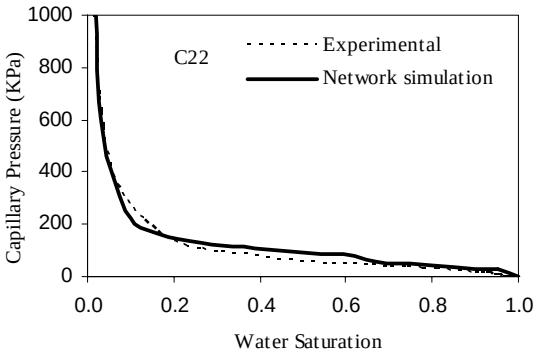

Figure 12: Comparison of the measured capillary pressure curve of carbonate C22 with simulation results.

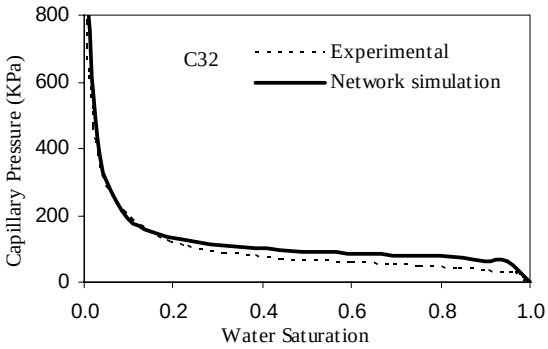

Figure 13: Comparison of the measured capillary pressure curve of carbonate C32 with simulation results.

The surface relaxivities used in the simulation were also selected to match the experimental data, surface relaxivity values of 2.8μm/s and 2.1μm/s were used for C22 and C32 networks respectively. The normalized magnetization decays of the networks and experimental data of both samples are consistent as shown in Figures 14a and 15a. The magnetization of the limestone (MB03 and MB11) and carbonates (C22 and C32) decay in the fast diffusion limit, i.e. ($\rho r/D$ <<1). This ratio ranges from 6×10^{-4} to 4.5×10^{-3} where r is determined as the average radius of the network elements, hence surface relaxation dominates.

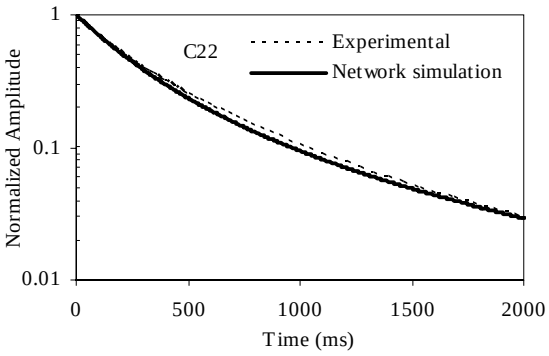

Figure 14a: Comparison of magnetization decays of the experimental data of C22 with simulation results of the tuned network.

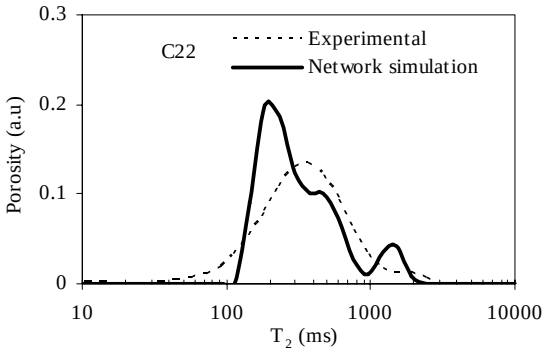

Figure 14b: The inverted T_2 distributions from the magnetization decays of C22 shown in Figure 14a.

The relaxation rate is controlled by the surface area to volume ratio of the network elements. Thus, the differences observed between the experimental and the simulated magnetization decays and T_2 distributions limestone (MB03 and MB11) and carbonates (C22 and C32) are attributed to geometrical effects (pore sizes and surface areas) inferring that the tuned network did not fully capture the pore sizes and surface areas of the actual porous medium.

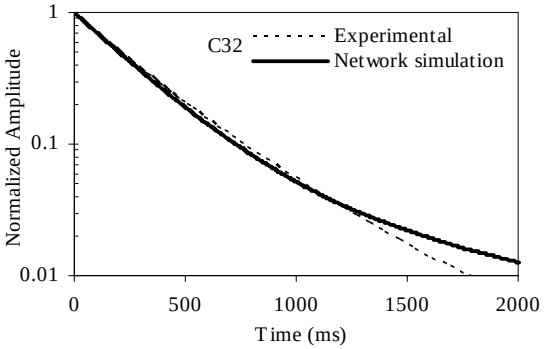

Figure 15a: Comparison of magnetization decays of the experimental data of C32 with simulation results of the tuned network.

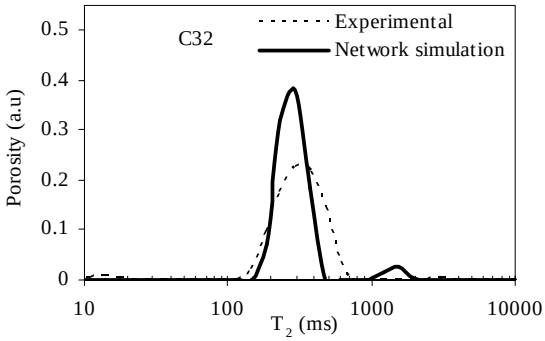

Figure 15b: The inverted T_2 distributions from the magnetization decays of C32 shown in Figure 15a.

CONCLUSIONS

In this work, we have been able to successfully compare magnetization decays and T_2 distributions of brine in networks extracted using the maximal ball method (Silin and Patzek, 2006; Al-Kharusi and Blunt, 2007; Dong, 2007) and micro CT images of sand packs within a good degree of accuracy. The experimental T_2 distribution of the sand packs and those of the micro-CT images are wider than the T_2 distribution of the networks which is attributable to the fact that some fine details of the pore structure were lost during network extraction. For the Bentheimer sandstone, predicted permeability and T_2

distribution of the tuned network are similar inferring that the network is identical both in geometry (pore sizes and surface areas) and topology to the real rock. However for carbonates, tuning elements' properties of a known network to match experimental capillary pressure resulted in differences in the comparison of the predicted permeability and T_2 distributions with experimental data. The differences observed in the experimental and the simulated T_2 distributions is more likely to be attributed to geometrical effects (pore sizes and surface areas) than topological differences since the walkers diffuse in fast diffusion limits which is governed by the surface area to volume ratio of the network elements. While the differences observed in the experimental and predicted permeabilities are as a result of both geometrical effects and topology. For carbonates, the tuning algorithm (Valvatne and Blunt, 2004) requires additional information about the pore space such as surface areas and pore sizes. As such, we believe that by combining this algorithm with other independent sources of information such as synchrotron micro CT images will further assist in obtaining better networks. This work highlights some of the challenges involved in obtaining networks that are geometrically and topologically identical to carbonates.

ACKNOWLEDGEMENTS

The members of the Imperial College consortium on Pore-Scale Modelling (BHP, Eni JOGMEC, Saudi Aramco, Schlumberger, Shell, Statoil, Total, the U.K. Department of Trade and Industry and the EPSRC) are thanked for their financial support. We will also like to express our gratitude to Reslab for allowing us to measure NMR response and capillary pressures at their Laboratory. Olumide Talabi will like to thank the Petroleum Technology Development Fund of Nigeria for Financial Support. Martin Fernø would like to acknowledge the Royal Norwegian Research Council for research funding.

REFERENCES

Al-Kharusi, A.S. and Blunt, M.J., 2007. Network extraction from sandstone and carbonate pore space images. Journal of Petroleum Science and Engineering 56: 219-231.

Arns, C., Knackstedt, M., Pinczewski, W. V. and N. Martys, 2004, Virtual permeametry on microtomographic images, J. Petroleum Science and Engineering, 45, 41-46.

Bergman, D. J., Dunn, K. J., Schwartz, L. M., and Mitra, P. P., 1995. Self-Diffusion in a Periodic Porous Medium: A Comparison of Different Approaches, Phys. Rev. 51 (4), 3393-3400.

Chang, D., Vinegar, H., Moriss, C., and Straley, C. 1997, Effective porosity, producible fluid, and permeability in carbonates from NMR logging, Log Analyst 38, 60-72.

Chen, S., Georgi, D., Fang, S., Salyer, J., and Shorey, D., 1999. Optimization of NMR Logging Acquisition and Processing: SPE 56766, presented at SPE 74th Annual Conference and Technical Exhibition (ATCE), Houston, Texas.

Dong, H., 2007. Micro CT imaging and pore network extraction, PhD thesis, Department of Earth Science and Engineering, Imperial College London. http://www3.imperial.ac.uk/earthscienceandengineering/research/perm.

Hazlett, R.D., 1995. Simulation of capillary-dominated displacements in microtomographic images of reservoir rocks. Transport Porous Media 20, 21–35.

Hinedi, Z. R., Chang, A. C., Anderson, M. A. and D. B. Borchardt, 1997, Quantification of microporosity by nuclear magnetic resonance relaxation of water imbibed in porous media, Water Resources. Research, 33, 2697–2704.

Lerdahl, T. R., P. E. Øren, and S. Bakke, 2000, A Predictive Network Model for Three-Phase Flow in Porous Media, proceedings of the SPE/DOE Symposium on Improved Oil Recovery, SPE 59311, Soc. of Petroleum Engineers, Tulsa.

Liaw, H., Kulkarni, R., Chen, S., and A. Ted Watson, 1996. Characterization of fluid distributions in porous media by NMR techniques, AIChE 42 (2), 538-546.

Okabe, H. and Blunt, J. M., 2004, Prediction of permeability for porous media reconstructed using multiple-point statistics, Phys. Rev. E 70, 066135.

Okabe, H., Blunt, M., 2005. Pore space reconstruction using multiple point statistics. J. Pet. Sci. Eng. 46, 121–137.

Øren, P. E., Antonsen, F., Rueslatten, H. G. and S. Bakke, 2002. Numerical Simulations of NMR Responses for Improved Interpretations of NMR Measurements in Reservoir Rocks, SPE 77398, SPE Annual Technical Conference and Exhibition, San Antonio, Texas, 2002.

Ramakrishnan, T.S., Schwartz, L.M., Fordham, E.J., Kenyon, W.E., and Wilkinson, D.J., 1999, Forward models for nuclear magnetic resonance in carbonate rocks, Log Analyst 40, 260-270.

Silin, D.B., Jin, G. and Patzek, T.W., 2003. Robust Determination of Pore Space Morphology in Sedimentary Rocks, SPE 84296, Proceedings of SPE Annual Technical Conference and Exhibition, Denver, Colorado, U.S.A.

Silin, D. and Patzek, T., 2006. Pore space morphology analysis using maximal inscribed spheres. Physica A, 371: 336-360.

Toumelin, E., 2002. Monte Carlo simulations of NMR measurements in carbonate rocks under a constant magnetic field gradient. Master's thesis, University of Texas at Austin.

Valvatne, P. H., 2003. Predictive pore-scale modelling of multiphase flow, PhD thesis, Department of Earth Science and Engineering, Imperial College London. http://www3.imperial.ac.uk/earthscienceandengineering/research/perm;

Valvatne, P.H. and Blunt, M.J., 2003. Predictive Pore-scale Network Modeling, SPE 84550, SPE Annual Technical Conference and Exhibition, Denver, Colorado, 2003.

Valvatne, P.H. and Blunt, M.J., 2004. Predictive Pore-scale Modeling of Two-phase Flow in Mixed Wet Media. Water Resources Research, 40, W07406.

Vogel, H. J., A numerical experiment on pore size, pore connectivity, water retention, permeability, and solute transport using network models, European Journal of Soil Science, 51, 99-105, 2000.